2024 European Control Conference (ECC)
June 25-28, 2024. Stockholm, Sweden

Global Exponential Saturated Output Feedback Design With Sign-Indefinite Quadratic Forms

Santiago Pantano Calderón, Sophie Tarbouriech, *Senior Member, IEEE*, Luca Zaccarian, *Fellow, IEEE*

Abstract— **This paper deals with the design of a dynamic output feedback controller of the same order as the plant. The plant under consideration is a linear system subject to saturating input and exponentially stable in open loop. The design technique takes advantage of a non-quadratic Lyapunov function involving sign-indefinite quadratic forms, which allows exploiting additional degrees of freedom with respect to a classical quadratic form. The design conditions, combining adequate changes of variables and several sector conditions, are stated in the form of linear matrix inequalities ensuring global exponential stability of the closed-loop system, in addition to a guaranteed prescribed local exponential convergence rate, typically selected as faster than the open-loop plant exponential convergence rate.**

I. Introduction

In practice, the safety, physical or technological constraints generally lead to magnitude limitations on the actuators (even on the sensors) of the control systems. It is then well-known that the negligence of such limitations may conduct to catastrophic behavior (see, for example, [12]). Several constructive methods based on linear matrix inequalities (LMI) conditions associated to convex optimization problem have been proposed to design control laws and anti-windup loops (see, for example, [5], [13], [14] and the references therein). A common feature of these works is the consideration of classical quadratic Lyapunov function to certify the closed-loop stability, associated with adequate ways to embed the saturation nonlinearity. The results based on quadratic Lyapunov functions may be conservative (see, for example, the discussion in [14, Section 4.4.1.1] or in [13, Example 3.3]).

It is important to recall that the design of a dynamic output controller of the same order of the linear plant is convex based on congruence transformations and the use of a quadratic Lyapunov function [10]. In the context of linear systems subject to input saturation, this kind of results have been extended by adding a static anti-windup loop to the dynamic output controller to derive convex conditions [6], [2], [4]. The objective of the current paper is to complete these results by considering a more general Lyapunov function, namely a non-quadratic Lyapunov function involving sign-indefinite quadratic forms introduced in [9] for the analysis case only. Later, the analysis results were extended to the case where a local stabilizer is given, in which the designs of static anti-windup loops ensuring global [8] and regional [7] stability properties of the anti-windup augmented feedback are presented. This paper further extends the use of sign-indefinite matrices to propose sufficient and less conservative LMI conditions allowing to synthesize the whole set of matrices of a dynamic output feedback controller including a static anti-windup loop. The convex conditions obtained guarantee global exponential stability of the closed loop, recalling that global exponential stability can only be provided under intuitive necessary conditions discussed in [11]. Furthermore, it is worth to emphasize that the conditions to design only the anti-windup loop proposed in [7], [8] were not convex, whereas the design conditions of the complete dynamic controller proposed in this note are. The design conditions combine the use of sign-indefinite quadratic forms, appropriate changes of variables inspired from [10] and generalized sector conditions involving the deadzone nonlinearity and its directional time derivative. The proposed LMI conditions allow to compute the matrices defining the dynamic output feedback controller ensuring global exponential stability and a minimum convergence rate. Also, point out that the guaranteed convergence rate is a local property in the sense that is only ensured when the input saturation is inactive.

The paper is organized as follows. Section II introduces the system under consideration and the dynamic controller with anti-windup loop to be synthesized. Section III presents the main result based on the use of a sign-indefinite quadratic form and appropriate changes of variables. Two numerical applications are reported in Section IV and the proof of the global exponential stability conditions is given in Section V. Finally, some concluding remarks and perspectives are discussed in Section VI.

Notation: M^T is the transpose of the matrix M and $M^{-\mathsf{T}}$ the transpose of the invertible matrix M^{-1}. Define $\text{He}\,(M) = M + M^\mathsf{T}$. Let M be a constant matrix and $\mathbf{M}$ an optimization decision variable. $\mathbb{R}^m$ is the Euclidean space of dimensions m. $\mathbb{D}^m$ ($\mathbb{D}^m_{>0}$) is the set of diagonal (positive-definite) matrices of dimension $m \times m$. $\mathbb{S}^m$ ($\mathbb{S}^m_{>0}$) is the set of symmetric (positive-definite) matrices of dimension $m \times m$. Given any matrix $M \in \mathbb{R}^{m\times m}$, $\lambda(M)$ is the set of eigenvalues of M, $\lambda_{\min}(M)$ the minimum eigenvalue of M and $\lambda_{\max}(M)$ the maximum eigenvalue of M. Finally, I_m is the identity matrix of dimensions $m\times m$ and 0 is the null matrix of appropriate dimensions.

S. Pantano Calderón (corresponding author), is with LAAS-CNRS, University of Toulouse, CNRS, Toulouse, France and also with the Department of Electrical and Computer Engineering, INSA Toulouse, France (e-mail: spantanca@laas.fr).
S. Tarbouriech is with LAAS-CNRS, University of Toulouse, CNRS, Toulouse, France (e-mail: tarbour@laas.fr).
L. Zaccarian is with LAAS-CNRS, University of Toulouse, CNRS, Toulouse, France and also with the Department of Industrial Engineering, University of Trento, Italy (e-mail: zaccarian@laas.fr).

II. System Definition

Consider the linear plant subject to input saturation

$$\left| \begin{array}{rcl} \dot{x}_p &=& A_p x_p + B_p \text{sat}(u) \\ y &=& C_p x_p \end{array} \right. , \tag{1}$$

with state $x_p \in \mathbb{R}^n$ and output $y \in \mathbb{R}^m$. A plant-order dynamic output feedback controller with anti-windup compensation is designed in this note, with

$$\left| \begin{array}{rcl} \dot{x}_c &=& A_c x_c + B_c y + E_c \text{dz}(u) \\ u &=& C_c x_c + D_c y \end{array} \right. , \tag{2}$$

where state $x_c \in \mathbb{R}^n$ and output $u \in \mathbb{R}^m$. Denote by $u \rightarrow \text{sat}(u)$ the decentralized symmetric saturation function, with

$$\text{sat}_i(u_i) := \max\{-\underline{u}_i, \min\{\bar{u}_i, u_i\}\}$$

for all $i = 1, \cdots, m$, where $\bar{u}_i > 0$ is the upper saturation limit and $\underline{u}_i > 0$ is the (absolute value of the) lower saturation limit. Introduce the deadzone function $\text{dz}(u) := u - \text{sat}(u)$, in such a way that the term $E_c \text{dz}(u)$ plays the role of the anti-windup compensator component. With these definitions, let A_c, B_c, C_c, D_c and E_c be the controller state-space model and anti-windup gain matrices to be designed.

Then, the closed-loop system between (1) and (2) can be compactly written as

$$\left| \begin{array}{rcl} \dot{x} &=& Ax + B\text{dz}(u) \\ u &=& Cx \end{array} \right. , \tag{3}$$

with $x := \begin{bmatrix} x_p^\mathsf{T} & x_c^\mathsf{T} \end{bmatrix}^\mathsf{T}$ and

$$\left[\begin{array}{c|c} A & B \\ \hline C & - \end{array} \right] = \left[\begin{array}{cc|c} A_p + B_p D_c C_p & B_p C_c & -B_p \\ B_c C_p & A_c & E_c \\ \hline D_c C_p & C_c & - \end{array} \right].$$

This note aims to propose a LMI-based method allowing to compute the dynamic output feedback controller (2) ensuring the two following properties:

1. Global exponential stability of the origin for the saturated closed loop (3).
2. Matrix A above satisfies a prescribed spectral abscissa of $-\alpha < 0$.

Note that the condition on the spectral abscissa of A in (3) ensures desirable local exponential stability with convergence rate α. Such a convergence rate is clearly enjoyed by small-signal responses that do not activate the saturation nonlinearity. Furthermore, notice that having A_p Hurwitz is a necessary condition to obtain global exponential stability for (3) due to the presence of the saturation limits and the resulting limitations of bounded stabilization [11].

III. Sign-Indefinite Quadratic Certificates

Define the extended state vector

$$\eta = \begin{bmatrix} x^\mathsf{T} & \text{dz}(Cx)^\mathsf{T} \end{bmatrix}^\mathsf{T}.$$

Then, the linear dynamic controller synthesis of this letter can be based on the Sign-Indefinite Quadratic form

$$V(x) := \eta^\mathsf{T} P \eta = \eta^\mathsf{T} \begin{bmatrix} P_{11} & P_{12} \\ P_{12}^\mathsf{T} & P_{22} \end{bmatrix} \eta, \tag{4}$$

with $P_{11} > 0$. Notice that V is locally positive-definite if P_{11} is positive-definite while P_{22} may be sign-indefinite, reducing conservativeness as compared to solutions using the classic quadratic forms $x^\mathsf{T} Q x$ requiring positive-definiteness of Q, as in [2], [4], [13]. Note that (4) is nonquadratic in x due to the piecewise affine dependence on x of the vector η. Introduce the full-rank matrices $\mathbf{X}, \mathbf{Y} \in \mathbb{S}^n_{>0}$, $\hat{X}, \hat{Y} \in \mathbb{S}^n_{>0}$ and $M, N \in \mathbb{R}^{n \times n}$ such that

$$P_{11} = \begin{bmatrix} \mathbf{X} & M \\ M^\mathsf{T} & \hat{X} \end{bmatrix}, \quad P_{11}^{-1} = \begin{bmatrix} \mathbf{Y} & N \\ N^\mathsf{T} & \hat{Y} \end{bmatrix}. \tag{5}$$

Using (5) and the fact that $P_{11} P_{11}^{-1} = P_{11}^{-1} P_{11} = I_n$, it can be seen that (5) holds for suitable selections of $\hat{X}$ and $\hat{Y}$ if and only if

$$\mathbf{XY} + MN^\mathsf{T} = \mathbf{YX} + NM^\mathsf{T} = I_n. \tag{6}$$

More specifically, under (5) and (6), the following symmetric selections for $\hat{X}$ and $\hat{Y}$ may be computed:

$$\begin{array}{rcl} \hat{X} &=& -M^\mathsf{T} \mathbf{Y} N^{-\mathsf{T}} \\ &=& -N^{-1}(\mathbf{Y} - \mathbf{YXY}) N^{-\mathsf{T}}, \\ \hat{Y} &=& -M^{-1} \mathbf{X} N \\ &=& -M^{-1}(\mathbf{X} - \mathbf{XYX}) M^{-\mathsf{T}}. \end{array} \tag{7}$$

Following similar derivations to those in [10], parametrize the controller matrices in (2) as

$$\begin{array}{rcl} A_c &=& M^{-1}\big(\hat{\mathbf{A}}_c - \mathbf{X}(A_p + B_p \hat{\mathbf{D}}_c C_p)\mathbf{Y} \\ && -M B_c C_p \mathbf{Y} - \mathbf{X} B_p C_c N^\mathsf{T}\big) N^{-\mathsf{T}}, \\ B_c &=& M^{-1}\big(\hat{\mathbf{B}}_c - \mathbf{X} B_p \hat{\mathbf{D}}_c\big), \\ C_c &=& \big(\hat{\mathbf{C}}_c - \hat{\mathbf{D}}_c C_p \mathbf{Y}\big) N^{-\mathsf{T}}, \\ D_c &=& \hat{\mathbf{D}}_c \\ E_c &=& M^{-1}\big(\hat{\mathbf{E}}_c + \mathbf{X} B_p \mathbf{S}\big) \mathbf{S}^{-1}. \end{array} \tag{8}$$

and the remaining entries in (4) as

$$\begin{array}{rcl} P_{12} &=& \begin{bmatrix} \mathbf{Y} & I_n \\ N^\mathsf{T} & 0 \end{bmatrix}^{-\mathsf{T}} \begin{bmatrix} \mathbf{W} \\ \mathbf{Z} \end{bmatrix} \mathbf{S}^{-1}, \\ P_{22} &=& \mathbf{S}^{-1} \hat{\mathbf{P}}_{22} \mathbf{S}^{-1}. \end{array} \tag{9}$$

With the parametrization above, the bold matrices $\hat{\mathbf{A}}_c \in \mathbb{R}^{n \times n}$, $\hat{\mathbf{B}}_c \in \mathbb{R}^{n \times m}$, $\hat{\mathbf{C}}_c \in \mathbb{R}^{m \times n}$, $\hat{\mathbf{D}}_c \in \mathbb{R}^{m \times m}$, $\hat{\mathbf{E}}_c \in \mathbb{R}^{n \times m}$, $\hat{\mathbf{P}}_{22} \in \mathbb{S}^m$, $\mathbf{S} \in \mathbb{D}^m_{>0}$, $\mathbf{W} \in \mathbb{R}^{n \times m}$ and $\mathbf{Z} \in \mathbb{R}^{n \times m}$ are the decision variables of the convex LMI-based synthesis formulated in the next theorem, which allows designing the linear dynamic stabilizing controller (2) for plant (1).

Theorem 1: Given a desired convergence rate $\alpha \geq 0$, if there exist matrices $\mathbf{X} \in \mathbb{S}^n_{>0}$, $\mathbf{Y} \in \mathbb{S}^n_{>0}$, $\mathbf{W} \in \mathbb{R}^{n \times m}$, $\mathbf{Z} \in \mathbb{R}^{n \times m}$, $\hat{\mathbf{P}}_{22} \in \mathbb{S}^m$, $\mathbf{S} \in \mathbb{D}^m_{>0}$, $\hat{\mathbf{A}}_c \in \mathbb{R}^{n \times n}$, $\hat{\mathbf{B}}_c \in \mathbb{R}^{n \times m}$, $\hat{\mathbf{C}}_c \in \mathbb{R}^{m \times n}$, $\hat{\mathbf{D}}_c \in \mathbb{R}^{m \times m}$, $\hat{\mathbf{E}}_c \in \mathbb{R}^{n \times m}$, $\hat{\mathbf{T}}_{pp} \in \mathbb{S}^n$, $\hat{\mathbf{T}}_{pc} \in \mathbb{R}^{n \times n}$ and $\hat{\mathbf{T}}_{cc} \in \mathbb{S}^n$ satisfying

$$\hat{T} = \begin{bmatrix} \hat{\mathbf{T}}_{pp} & \hat{\mathbf{T}}_{pc} \\ \hat{\mathbf{T}}_{pc}^{\mathsf{T}} & \hat{\mathbf{T}}_{cc} \end{bmatrix} > 0, \quad (10)$$

$$\Psi_1 = \mathrm{He}\left(\begin{bmatrix} \frac{1}{2}\mathbf{Y} & 0 & \mathbf{W} \\ I_{n_p} & \frac{1}{2}\mathbf{X} & \mathbf{Z} \\ -\hat{\mathbf{C}}_c & -\hat{\mathbf{D}}_c C_p & \frac{1}{2}\hat{\mathbf{P}}_{22} + \mathbf{S} \end{bmatrix}\right) > 0 \quad (11)$$

and conditions (12) and (13) at the bottom of this page, then the origin of (3) with the controller state-space model matrices A_c, B_c, C_c, D_c and E_c as selected in (8) is globally exponentially stable. Moreover, the eigenvalues of A in (3) have real part smaller than $-\alpha$.

Proof: The proof of Theorem 1 is presented in section V.

IV. Numerical examples and simulations

The solution proposed in Theorem 1 is applied to two numerical examples.

A. Single input example

Consider the SISO plant with state-space model matrices

$$A_p = \begin{bmatrix} -3 & 1 \\ 1 & -2 \end{bmatrix}, \quad B_p = \begin{bmatrix} 1 \\ 0.5 \end{bmatrix}, \quad C_p = \begin{bmatrix} 1 & 1 \end{bmatrix}, \quad (14)$$

and $\bar{u} = 2$, $M = I_n$. In a first case, take $\alpha = 0.1$. The controller state-space model matrices obtained from Theorem 1 are then

$$A_c = \begin{bmatrix} -2.2293 & 0.7734 \\ 1.5373 & -2.2945 \end{bmatrix}, \quad B_c = \begin{bmatrix} -1.0674 \\ -2.4750 \end{bmatrix}, \quad C_c = \begin{bmatrix} -0.0196 & 0.0567 \end{bmatrix}, \quad D_c = 0.6973, \quad E_c = \begin{bmatrix} 10.3178 \\ 9.4127 \end{bmatrix}, \quad (15)$$

while the matrix P determined from (5), (7), (9) has eigenvalues

$$\lambda(P) = \{2.8377 \cdot 10^3,\ 2.5999 \cdot 10^2,\ -8.5063 \cdot 10^{-3},\ 6.6814 \cdot 10^{-3},\ 7.1259 \cdot 10^{-4}\},$$

where there is a negative eigenvalue, showing that the optimizer exploits a sign-indefinite P for V in (4). Figure 1 shows the input-output response of (3) with the plant and controller matrices in (14) and (15), respectively, from the initial state

$$x_0 = \begin{bmatrix} -2.5 & -2.5 & 0 & 0 \end{bmatrix}^{\mathsf{T}},$$

carefully chosen to have an initial output $y_0 = -5$. It is possible to observe that the proposed controller synthesis eliminates the overshoot and reduces the settling time, as compared to the response obtained with the solution proposed in [13, Proposition 3.18], which is founded on positive-definite quadratic forms.

In a second case, let $\alpha = 1.5$. With this given desired convergence rate, the controller issued from the proposed procedure is

$$A_c = \begin{bmatrix} -2.7776 & 0.5282 \\ 0.6388 & -2.7664 \end{bmatrix}, \quad B_c = \begin{bmatrix} 0.4417 \\ -4.9914 \end{bmatrix}, \quad C_c = \begin{bmatrix} -0.0285 & 0.0439 \end{bmatrix}, \quad D_c = -0.0817, \quad E_c = \begin{bmatrix} 7.9591 \\ 6.1248 \end{bmatrix}, \quad (16)$$

whereas the solution exposed in [13, Proposition 3.18] is not able to find a feasible selection for the controller (2). Figure 2 shows the input-output response of the closed-loop (3) with the plant (14) and controller (16).

B. Multiple input example

The proposed controller design is now applied to a MIMO example based on [14, Example 4.3.2]. Let $\bar{u} = \begin{bmatrix} 1 & 1 \end{bmatrix}^{\mathsf{T}}$, $M = I_n$, $\alpha = 5 \cdot 10^{-3}$ and

$$A_p = \begin{bmatrix} -0.01 & 0 \\ 0 & -0.01 \end{bmatrix}, \quad B_p = \begin{bmatrix} 1 & 0 \\ 0 & 1 \end{bmatrix}, \quad C_p = \begin{bmatrix} -0.4 & 0.5 \\ -0.1 & 0.1 \end{bmatrix}. \quad (17)$$

For this plant, the optimizer produces a state-space model of the controller with

$$A_c = \begin{bmatrix} -0.6882 & 0 \\ 0 & -0.6882 \end{bmatrix}, \quad B_c = \begin{bmatrix} 8.4412 & -10.5515 \\ 2.1103 & -8.4412 \end{bmatrix}, \quad C_c = \begin{bmatrix} 0.0108 & 0 \\ 0 & 0.0108 \end{bmatrix}, \quad D_c = \begin{bmatrix} 0.7927 & -0.9909 \\ 0.1982 & -0.7927 \end{bmatrix}, \quad E_c = \begin{bmatrix} 6.0818 & 0 \\ 0 & 6.0818 \end{bmatrix}, \quad (18)$$

$$\Psi_2 = \mathrm{He}\left(\begin{bmatrix} A_p\mathbf{Y} + B_p\hat{\mathbf{C}}_c & A_p + B_p\hat{\mathbf{D}}_c C_p & 0 & 0 & -B_p\mathbf{S} & \mathbf{W} \\ \hat{\mathbf{A}}_c & \mathbf{X}A_p + \hat{\mathbf{B}}_c C_p & 0 & 0 & \hat{\mathbf{E}}_c & \mathbf{Z} \\ A_p\mathbf{Y} + B_p\hat{\mathbf{C}}_c & A_p + B_p\hat{\mathbf{D}}_c C_p & -\mathbf{Y} & -I_{n_p} & -B_p\mathbf{S} & 0 \\ \hat{\mathbf{A}}_c & \mathbf{X}A_p + \hat{\mathbf{B}}_c C_p & -I_{n_p} & -\mathbf{X} & \hat{\mathbf{E}}_c & 0 \\ \hat{\mathbf{C}}_c & \hat{\mathbf{D}}_c C_p & \mathbf{W}^{\mathsf{T}} + \hat{\mathbf{C}}_c & \mathbf{Z}^{\mathsf{T}} + \hat{\mathbf{D}}_c C_p & -\mathbf{S} & \hat{\mathbf{P}}_{22} \\ 0 & 0 & \hat{\mathbf{C}}_c & \hat{\mathbf{D}}_c C_p & -\mathbf{S} & -\mathbf{S} \end{bmatrix}\right) < 0 \quad (12)$$

$$\Psi_3 = \mathrm{He}\left(\begin{bmatrix} A_p\mathbf{Y} + B_p\hat{\mathbf{C}}_c + \alpha\mathbf{Y} & A_p + B_p\hat{\mathbf{D}}_c C_p + \alpha I_n & \hat{\mathbf{T}}_{pp} - \mathbf{Y} & \hat{\mathbf{T}}_{pc} - I_n \\ \hat{\mathbf{A}}_c + \alpha I_n & \mathbf{X}A_p + \hat{\mathbf{B}}_c C_p + \alpha\mathbf{X} & \hat{\mathbf{T}}_{pc}^{\mathsf{T}} - I_n & \hat{\mathbf{T}}_{cc} - \mathbf{X} \\ A_p\mathbf{Y} + B_p\hat{\mathbf{C}}_c + \alpha\mathbf{Y} & A_p + B_p\hat{\mathbf{D}}_c C_p + \alpha I_n & -\mathbf{Y} & -I_n \\ \hat{\mathbf{A}}_c + \alpha I_n & \mathbf{X}A_p + \hat{\mathbf{B}}_c C_p + \alpha\mathbf{X} & -I_n & -\mathbf{X} \end{bmatrix}\right) < 0 \quad (13)$$

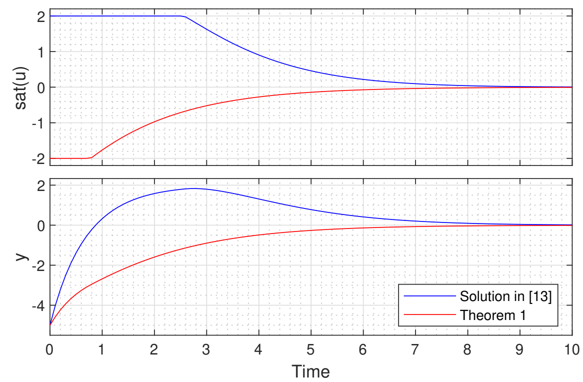

Fig. 1. Response of closed-loop (3) with plant (14) from the initial state $x_0 = \begin{bmatrix} -2.5 & -2.5 & 0 & 0 \end{bmatrix}^\mathsf{T}$. In red, response with controller (15). In blue, response obtained with the solution presented in [13, Proposition 3.18].

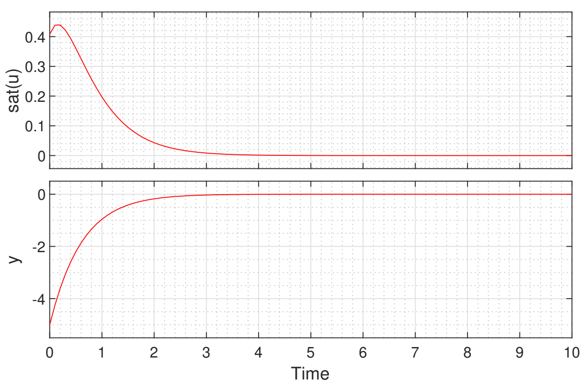

Fig. 2. Response of closed-loop (3) with plant (14) and controller (16) from the initial state $x_0 = \begin{bmatrix} -2.5 & -2.5 & 0 & 0 \end{bmatrix}^\mathsf{T}$.

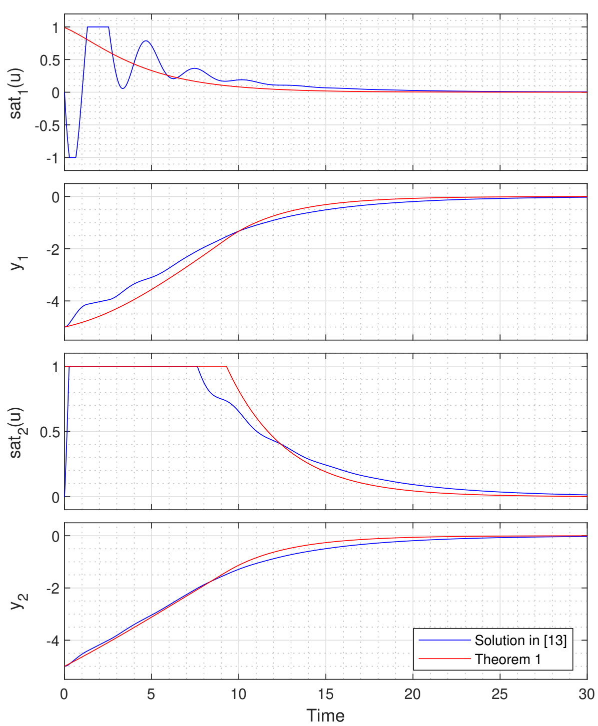

Fig. 3. Response of the closed-loop system (3) with plant (17) from the initial state $x_0 = \begin{bmatrix} -4.5455 & -13.6364 & 0 & 0 \end{bmatrix}^\mathsf{T}$. In red, response with the controller synthesized (18). In blue, response obtained with the solution presented in [13, Proposition 3.18].

and a positive-definite matrix P with eigenvalues

$$\lambda(P) = \{2.6155 \cdot 10^{-3},\ 2.4781 \cdot 10^{-1},\ 2.2429 \cdot 10^{2},\\ 2.2429 \cdot 10^{2},\ 2.6155 \cdot 10^{-3},\ 2.4781 \cdot 10^{-1}\}.$$

Figure 3 reports on the input-output response of (3) with the state-space matrices in (17) and (18) from the initial state

$$x_0 = \begin{bmatrix} -4.5455 & -13.6364 & 0 & 0 \end{bmatrix}^\mathsf{T}.$$

Analogous to the Example IV-A, these initial conditions are chosen in such a way that $y_0 = \begin{bmatrix} -5 & -5 \end{bmatrix}^\mathsf{T}$. Notice that, despite the positive-definiteness condition of P, a smoother and faster convergence of outputs y_1 and y_2 is obtained, as compared to the response found with the method suggested in [13, Proposition 3.18] using a classic quadratic Lyapunov function.

V. Proof of Theorem 1

This section addresses the rationale behind the global exponential stability certificate presented in Section III, thus the Proof of Theorem 1. To this end, first, consider the following preliminary facts (see [9, Facts 3-5]).

Global Sector Condition: For any $T_1 \in \mathbb{D}^m_{>0}$, it holds that for all $x \in \mathbb{R}^{2n}$ and all $u \in \mathbb{R}^m$,

$$\mathrm{dz}\,(u)^\mathsf{T} T_1(u - \mathrm{dz}\,(u)) \geq 0. \tag{19}$$

Derivative of the Deadzone: For any $T_2 \in \mathbb{D}^m$, $T_3 \in \mathbb{D}^m$ and for almost all $x \in \mathbb{R}^{2n}$,

$$\mathrm{dz}\,(Cx)^\mathsf{T} T_2(C\dot{x} - \dot{\mathrm{dz}}\,(Cx)) \equiv 0, \tag{20}$$

$$\dot{\mathrm{dz}}\,(Cx)^\mathsf{T} T_3(C\dot{x} - \dot{\mathrm{dz}}\,(Cx)) \equiv 0, \tag{21}$$

where $\dot{x}$ is a shortcut for $Ax + B\mathrm{dz}\,(u)$ as for (3) and $\dot{\mathrm{dz}}\,(Cx)$ denotes the time derivative of $x \to \mathrm{dz}\,(Cx)$, which is well defined for almost all values of $x \in \mathbb{R}^{2n}$. Define the extended state-vector

$$\upsilon = \begin{bmatrix} x^\mathsf{T} & \dot{x}^\mathsf{T} & \mathrm{dz}\,(u)^\mathsf{T} & \dot{\mathrm{dz}}\,(u)^\mathsf{T} \end{bmatrix}^\mathsf{T}$$

and notice that, from dynamics (3), for any matrix K,

$$\upsilon^\mathsf{T} K(Ax + B\mathrm{dz}\,(u) - \dot{x}) = 0. \tag{22}$$

Now, let V in (4) be a Lyapunov function candidate. With selection (5), introduce the nonsingular matrix

$$\Pi = \begin{bmatrix} \mathbf{Y} & I_n \\ N^\mathsf{T} & 0 \end{bmatrix}, \tag{23}$$

for which the property

$$\Pi^\mathsf{T} P_{11} = \begin{bmatrix} I_n & 0 \\ \mathbf{X} & M \end{bmatrix}$$

is easily verified by substitution. Due to matrix Π in (23), using $\hat{X} = -N^{-1}\mathbf{Y}M$, which is an allowable selection as established in (7), it is immediate to show that

$$\Pi^\mathsf{T} P_{11} \Pi = \begin{bmatrix} \mathbf{Y} & I_n \\ I_n & \mathbf{X} \end{bmatrix}. \tag{24}$$

Select the remaining entries of P in (4) as in (7) so that, with the notation above,

$$\Pi^{\mathsf{T}} P_{12}\mathbf{S} = \begin{bmatrix}\mathbf{W}\\ \mathbf{Z}\end{bmatrix}, \quad \mathbf{S}P_{22}\mathbf{S} = \hat{\mathbf{P}}_{22}. \tag{25}$$

To prove now the positive-definiteness and radial unboundness of V, select $T_1 = \mathbf{S}^{-1}$ in (19). Then, the property

$$\begin{aligned} V(x) &\geq V(x) - 2\,\mathrm{dz}\,(Cx)\,\mathbf{S}^{-1}(Cx - \mathrm{dz}\,(Cx)) \\ &= \eta^{\mathsf{T}}\tilde{\Psi}_1\eta > 0 \end{aligned} \tag{26}$$

holds if

$$\tilde{\Psi}_1 = \mathrm{He}\left(\begin{bmatrix}\frac{1}{2}P_{11} & P_{12}\\ -\mathbf{S}^{-1}C & \frac{1}{2}P_{22}+\mathbf{S}^{-1}\end{bmatrix}\right) > 0. \tag{27}$$

Since both Π and $\mathbf{S}$ are nonsingular, then (27) holds if and only if

$$\begin{aligned} &\begin{bmatrix}\Pi & 0\\ 0 & \mathbf{S}\end{bmatrix}^{\mathsf{T}} \tilde{\Psi}_1 \begin{bmatrix}\Pi & 0\\ 0 & \mathbf{S}\end{bmatrix} \\ &\quad = \mathrm{He}\left(\begin{bmatrix}\frac{1}{2}\mathbf{Y} & 0 & \mathbf{W}\\ I_{n_p} & \frac{1}{2}\mathbf{X} & \mathbf{Z}\\ -\hat{\mathbf{C}}_c & -\hat{\mathbf{D}}_cC_p & \frac{1}{2}\hat{\mathbf{P}}_{22}+\mathbf{S}\end{bmatrix}\right) > 0, \end{aligned}$$

whose expression stems from (24), (25) and which is positive definite due to (11). Therefore, using

$$|\eta|^2 \leq |x|^2 + |Cx|^2 \leq (1+|C|^2)|x|^2$$

together with $\tilde{\Psi}_1 > 0$, it holds that

$$\begin{aligned} &\lambda_{\min}\left(\tilde{\Psi}_1\right)|x|^2 \leq V(x) \\ &\qquad \leq \lambda_{\max}(P)|\eta|^2 \leq \lambda_{\max}(P)(1+|C|^2)|x|^2, \end{aligned} \tag{28}$$

which implies positive-definiteness and radial unboundedness of V.

To prove now that $\dot{V}(x) < 0$ for almost all $x \in \mathbb{R}^{2n}$, first, observe that selections (8) can be inverted as

$$\begin{aligned} \hat{\mathbf{A}}_c &= \mathbf{X}(A_p + B_p\hat{\mathbf{D}}_cC_p)\mathbf{Y} + MB_cC_p\mathbf{Y} \\ &\qquad + \mathbf{X}B_pC_cV^{\mathsf{T}} + MA_cN^{\mathsf{T}}, \\ \hat{\mathbf{B}}_c &= \mathbf{X}B_p\hat{\mathbf{D}}_c + MB_c, \\ \hat{\mathbf{C}}_c &= \hat{\mathbf{D}}_cC_p\mathbf{Y} + C_cN^{\mathsf{T}}, \\ \hat{\mathbf{D}}_c &= D_c, \\ \hat{\mathbf{E}}_c &= ME_c\mathbf{S} - \mathbf{X}B_p\mathbf{S}. \end{aligned}$$

With the expressions above and after some cumbersome calculations exploiting (23)-(25), it is possible to show that

$$\begin{aligned} \Pi^{\mathsf{T}}P_{11}A\Pi &= \begin{bmatrix}A_p\mathbf{Y} + B_p\hat{\mathbf{C}}_c & A_p + B_p\mathbf{D}_cC_p\\ \hat{\mathbf{A}}_c & \mathbf{X}A_p + \hat{\mathbf{B}}_cC_p\end{bmatrix}, \\ \Pi^{\mathsf{T}}P_{11}B\mathbf{S} &= \begin{bmatrix}-B_p\mathbf{S}\\ \hat{\mathbf{E}}_c\end{bmatrix}, \\ C\Pi &= \begin{bmatrix}\hat{\mathbf{C}}_c & \hat{\mathbf{D}}_cC_p\end{bmatrix}. \end{aligned} \tag{29}$$

Now, consider selecting $T_2 = T_3 = \mathbf{S}^{-1}$ in (20), (21) and

$$K = \begin{bmatrix}0 & P_{11} & -P_{12} - C^{\mathsf{T}}\mathbf{S}^{-1} & -C^{\mathsf{T}}\mathbf{S}^{-1}\end{bmatrix}^{\mathsf{T}}$$

in (22). Then, the following holds:

$$\begin{aligned} 0 &\leq \tilde{\psi}_{2,1}(x) = 2\,\mathrm{dz}\,(Cx)^{\mathsf{T}}\,\mathbf{S}^{-1}(Cx - \mathrm{dz}\,(Cx)) \\ &= \upsilon^{\mathsf{T}}\mathrm{He}\left(\begin{bmatrix}0\\0\\ \mathbf{S}^{-1}\\0\end{bmatrix}\begin{bmatrix}C & 0 & -I_m & 0\end{bmatrix}\right)\upsilon, \\ 0 &= \tilde{\psi}_{2,2}(x) = 2\,\mathrm{dz}\,(Cx)^{\mathsf{T}}\,\mathbf{S}^{-1}(C\dot{x} - \dot{\mathrm{dz}}\,(Cx)) \\ &= \upsilon^{\mathsf{T}}\mathrm{He}\left(\begin{bmatrix}0\\0\\ \mathbf{S}^{-1}\\0\end{bmatrix}\begin{bmatrix}CA & 0 & CB & -I_m\end{bmatrix}\right)\upsilon, \\ 0 &= \tilde{\psi}_{2,3}(x) = 2\,\dot{\mathrm{dz}}\,(Cx)^{\mathsf{T}}\,\mathbf{S}^{-1}(C\dot{x} - \dot{\mathrm{dz}}\,(Cx)) \\ &= \upsilon^{\mathsf{T}}\mathrm{He}\left(\begin{bmatrix}0\\0\\0\\ \mathbf{S}^{-1}\end{bmatrix}\begin{bmatrix}CA & 0 & CB & -I_m\end{bmatrix}\right)\upsilon, \\ 0 &= \tilde{\psi}_{2,4}(x) = 2\,\upsilon^{\mathsf{T}}K(Ax + B\mathrm{dz}\,(u) - \dot{x}) \\ &= \upsilon^{\mathsf{T}}\mathrm{He}\left(\begin{bmatrix}0\\ P_{11}\\ -P_{12}^{\mathsf{T}} - \mathbf{S}^{-1}C\\ -\mathbf{S}^{-1}C\end{bmatrix}\begin{bmatrix}A & -I_{2n} & B & 0\end{bmatrix}\right)\upsilon. \end{aligned}$$

Moreover, from (4) it may be computed

$$\begin{aligned} \dot{V}(x) &= 2\,\eta^{\mathsf{T}}P\begin{bmatrix}Ax + B\mathrm{dz}\,(u)\\ \dot{\mathrm{dz}}\,(Cx)\end{bmatrix} \\ &= \upsilon^{\mathsf{T}}\mathrm{He}\left(\begin{bmatrix}I_n & 0\\ 0 & 0\\ 0 & I_m\\ 0 & 0\end{bmatrix}P\begin{bmatrix}A & 0 & B & 0\\ 0 & 0 & 0 & I_m\end{bmatrix}\right)\upsilon, \end{aligned}$$

which allows upper bounding for $\dot{V}(x)$ for almost all $x \in \mathbb{R}^{2n}$ as

$$\begin{aligned} \dot{V}(x) &\leq \dot{V}(x) + \tilde{\psi}_{2,1}(x) + \tilde{\psi}_{2,2}(x) + \tilde{\psi}_{2,3}(x) + \tilde{\psi}_{2,4}(x) \\ &= \upsilon^{\mathsf{T}}\tilde{\Psi}_2\upsilon, \end{aligned} \tag{30}$$

with $\tilde{\Psi}_2$ given by

$$\begin{aligned} \tilde{\Psi}_2 &= \mathrm{He}\left(\begin{bmatrix}P_{11}A & 0 & P_{11}B & P_{12}\\ 0 & 0 & 0 & 0\\ P_{12}^{\mathsf{T}}A & 0 & P_{12}^{\mathsf{T}}B & P_{22}\\ 0 & 0 & 0 & 0\end{bmatrix}\right) \\ &\quad + \mathrm{He}\left(\begin{bmatrix}0\\0\\ \mathbf{S}^{-1}\\0\end{bmatrix}\begin{bmatrix}C & 0 & -I_m & 0\end{bmatrix}\right) \\ &\quad + \mathrm{He}\left(\begin{bmatrix}0\\0\\ \mathbf{S}^{-1}\\0\end{bmatrix}\begin{bmatrix}CA & 0 & CB & -I_m\end{bmatrix}\right) \end{aligned}$$

$$+\operatorname{He}\left(\begin{bmatrix}0\\0\\0\\\mathbf{S}^{-1}\end{bmatrix}\begin{bmatrix}CA & 0 & CB & -I_m\end{bmatrix}\right)$$

$$+\operatorname{He}\left(\begin{bmatrix}0\\P_{11}\\-P_{12}^{\mathsf T}-\mathbf{S}^{-1}C\\-\mathbf{S}^{-1}C\end{bmatrix}\begin{bmatrix}A & -I_{2n} & B & 0\end{bmatrix}\right)$$

$$=\operatorname{He}\left(\begin{bmatrix}P_{11}A & 0 & P_{11}B & P_{12}\\ P_{11}A & -P_{11} & P_{11}B & 0\\ \mathbf{S}^{-1}C & P_{12}^{\mathsf T}+\mathbf{S}^{-1}C & -\mathbf{S}^{-1} & P_{22}\\ 0 & \mathbf{S}^{-1}C & -\mathbf{S}^{-1} & -\mathbf{S}^{-1}\end{bmatrix}\right).$$

Exploiting again the invertibility of Π and $\mathbf{S}$, it holds that $\tilde\Psi_2 < 0$ if and only if

$$\begin{bmatrix}\Pi & 0 & 0 & 0\\ 0 & \Pi & 0 & 0\\ 0 & 0 & \mathbf{S} & 0\\ 0 & 0 & 0 & \mathbf{S}\end{bmatrix}^{\mathsf T}\tilde\Psi_2\begin{bmatrix}\Pi & 0 & 0 & 0\\ 0 & \Pi & 0 & 0\\ 0 & 0 & \mathbf{S} & 0\\ 0 & 0 & 0 & \mathbf{S}\end{bmatrix}$$

$$=\operatorname{He}\left(\begin{bmatrix}\Pi^{\mathsf T}P_{11}A\Pi & 0 & \Pi^{\mathsf T}P_{11}B\mathbf{S} & \Pi^{\mathsf T}P_{12}\mathbf{S}\\ \Pi^{\mathsf T}P_{11}A\Pi & -\Pi^{\mathsf T}P_{11}\Pi & \Pi^{\mathsf T}P_{11}B\mathbf{S} & 0\\ C\Pi & \mathbf{S}P_{12}^{\mathsf T}\Pi+C\Pi & -\mathbf{S} & \mathbf{S}P_{22}\mathbf{S}\\ 0 & C\Pi & -\mathbf{S} & -\mathbf{S}\end{bmatrix}\right)$$

is negative-definite. Using (25) and (29), it is immediate to check that the matrix above coincides with Ψ_2 in (12), which is negative-definite by assumption. Since $\tilde\Psi_2 < 0$, taking $\epsilon = -\lambda_{\max}\left(\tilde\Psi_2\right) > 0$, notice that, from (30),

$$\begin{aligned}\dot V(x) &= \left\langle \nabla V(x), Ax + B\mathrm{dz}\,(Cx)\right\rangle\\ &\le -\epsilon\,|x|^2.\end{aligned}$$

Therefore, applying Proposition 1 of [3], which fits because V in (4) is locally Lipschitz, it holds that

$$\left\langle \delta_v, Ax + B\mathrm{dz}\,(Cx)\right\rangle \le -\epsilon|x|^2,\quad \forall x\in\mathbb{R}^n, \forall \delta_v \in \partial V(x), \tag{31}$$

where $\partial V(x)$ denotes the Clarke generalized gradient of V at x. Hence, combining (31) with the quadratic upper and lower bounds of V in (28) and proceeding as in [1, Section 4.5] proves global exponential stability of the origin.

Finally, to prove that the spectral abscissa of A is smaller than $-\alpha$, it suffices to show that the matrix $\hat A := A + \alpha I_n$ is Hurwitz. Following a similar approach to [9, Proposition 2], introduce the matrix $T \in \mathbb{S}^{2n}_{>0}$ defined as

$$T = \Pi^{-\mathsf T}\hat T\Pi^{-1}.$$

with $\hat T$ defined as in (10). Then, using (24) and (29), observe that property (13) assumed in the theorem implies

$$\begin{bmatrix}\Pi & 0\\ 0 & \Pi\end{bmatrix}^{-\mathsf T}\Psi_3\begin{bmatrix}\Pi & 0\\ 0 & \Pi\end{bmatrix}^{-1} = \operatorname{He}\left(\begin{bmatrix}P_{11}\hat A & T - P_{11}\\ P_{11}\hat A & -P_{11}\end{bmatrix}\right) < 0,$$

which pre and postmultiplied by $\begin{bmatrix}x^{\mathsf T} & x^{\mathsf T}\hat A^{\mathsf T}\end{bmatrix}$ and its transpose reads

$$x^{\mathsf T}T\hat A x = x^{\mathsf T}T(A+\alpha I_{2n})x < 0,$$

proving that $\hat A$ is Hurwitz, thus completing the proof of Theorem 1. □

VI. Concluding comments

The paper addressed the design of a dynamic output controller including an anti-windup loop for global exponentially stable plants subject to input saturation. The designed controller is of the same order as the plant order. The design conditions are formulated as LMIs and re derived by combining the use of sign-indefinite quadratic forms, appropriate changes of variables inspired from [10] and generalized sector conditions involving the dead-zone nonlinearity and its directional time derivative. Furthermore, the proposed results pave the way for future works. In particular, it would be interesting to consider the case where the plant is exponentially unstable, leading to provide design conditions guaranteeing the regional exponential stability for the closed-loop system.

References

[1] F.H. Clarke, Y.S. Ledyaev, R.J. Stern, and P.R. Wolenski. *Nonsmooth Analysis and Control Theory*. Springer-Verlag, Berlin, Heidelberg, 1998.

[2] D. Dai, T. Hu, A.R. Teel, and L. Zaccarian. Output feedback design for saturated linear plants using deadzone loops. *Automatica*, 45(12):2917–2924, 2009.

[3] M. Della Rossa, R. Goebel, A. Tanwani, and L. Zaccarian. Piecewise structure of lyapunov functions and densely checked decrease conditions for hybrid systems. *Mathematics of Control, Signals, and Systems*, 33:123–149, 2021.

[4] G. Garcia, S. Tarbouriech, J.M. Gomes da Silva, and D. Eckhard. Finite $\mathcal{L}_2$ gain and internal stabilisation of linear systems subject to actuator and sensor saturations. *IET Control Theory & Applications*, 3:799–812(13), July 2009.

[5] T. Hu and Z. Lin. *Control systems with actuator saturation: analysis and design*. Birkhauser, Boston, 2001.

[6] T. Nguyen and F. Jabbari. Output feedback controllers for disturbance attenuation with actuator amplitude and rate saturation. In *Proceedings of the 1999 American Control Conference (Cat. No. 99CH36251)*, volume 3, pages 1997–2001 vol.3, 1999.

[7] S. Pantano Calderón, S. Tarbouriech, and L. Zaccarian. Local static anti-windup design with sign-indefinite quadratic forms. *IEEE Control Systems Letters*, 7:3090–3095, 2023.

[8] A. Priuli, S. Tarbouriech, and L. Zaccarian. Static linear anti-windup design with sign-indefinite quadratic forms. *IEEE Control Systems Letters*, 6:3158–3163, 2022.

[9] I. Queinnec, S. Tarbouriech, G. Valmorbida, and L. Zaccarian. Design of saturating state feedback with sign-indefinite quadratic forms. *IEEE Transactions on Automatic Control*, 67(7):3507–3520, 2022.

[10] C. Scherer, P. Gahinet, and M. Chilali. Multiobjective output-feedback control via LMI optimization. *IEEE Transactions on Automatic Control*, 42(7):896–911, 1997.

[11] E.D. Sontag. An algebraic approach to bounded controllability of linear systems. *International Journal of Control*, 39(1):181–188, 1984.

[12] G. Stein. Respect the unstable. *IEEE Control Systems Magazine*, 23(4):12–25, 2003.

[13] S. Tarbouriech, G. Garcia, J.M. Gomes da Silva Jr., and I. Queinnec. *Stability and stabilization of linear systems with saturating actuators*. Springer London, 2011.

[14] L. Zaccarian and A.R. Teel. *Modern Anti-windup Synthesis: Control Augmentation for Actuator Saturation*. Princeton Series in Applied Mathematics. Princeton University Press, 2011.